Generation of 20 GHz, sub-40 fs pulses at 960 nm via repetition-rate multiplication

M. S. Kirchner,[1,2,*] D. A. Braje,[2] T. M. Fortier,[2] A. M. Weiner,[3] L. Hollberg,[2] and S. A. Diddams[2]

[1]*Department of Physics, University of Colorado, 2000 Colorado Avenue, Boulder, Colorado 80309, USA*
[2]*National Institute of Standards and Technology, 325 Broadway MS 847, Boulder, Colorado 80305, USA*
[3]*Electrical and Computer Engineering, Purdue University, West Lafayette, Indiana 47907, USA*
**Corresponding author: mkirchne@boulder.nist.gov*

Received December 8, 2008; revised February 11, 2009; accepted February 12, 2009;
posted February 18, 2009 (Doc. ID 104897); published March 16, 2009

Optical filtering of a stabilized 1 GHz optical frequency comb produces a 20 GHz comb with ~40 nm bandwidth (FWHM) at 960 nm. Use of a low-finesse Fabry–Pérot cavity in a double-pass configuration provides a broad cavity coupling bandwidth ($\Delta\lambda/\lambda \approx 10\%$) and large suppression (50 dB) of unwanted modes. Pulse durations shorter than 40 fs with less than 2% residual amplitude modulation are achieved.

OCIS codes: 140.7090, 070.2615, 320.5540.

High-repetition-rate mode-locked lasers and their associated frequency combs are useful for applications such as communications and waveform generation [1–3], frequency synthesis [4], and the calibration of astronomical spectrographs [5,6]. Many of these applications require a stabilized frequency comb; however, for mode spacings above a few gigahertz, the spectral width required for frequency stabilization via self-referencing [7] is difficult to achieve because of the low pulse energy. As a solution, we begin with an octave-spanning self-referenced 1 GHz Ti:sapphire frequency comb and optically filter it to 20 GHz using an air-spaced Fabry–Pérot (FP) etalon in a double-pass configuration. The FP filtering approach, where a resonant cavity selects every Nth comb mode (increasing the repetition rate by a factor of N while decreasing the average power by a factor of N and pulse energy by N^2), has been well known for many years [8,9]. More recently the double-pass FP filtering approach has been implemented in fiber cavities over a narrow bandwidth ($\Delta\lambda/\lambda \approx 0.1\%$) [10]. We demonstrate that a double-pass FP filter cavity can support both broad coupling bandwidths ($\Delta\lambda/\lambda \approx 10\%$) and high suppression (greater than 50 dB in intensity) of off-resonant modes. We show sub-40 fs pulses at 960 nm, which to our knowledge are the shortest pulses produced at a 20 GHz rate. The residual amplitude modulation at 1 GHz on the 4.5 mW output is less than 2%. A semiconductor optical amplifier can be used to compensate for additional losses to maintain average power levels at the 5–10 mW level with only a small increase in pulse duration. This unique comb source with over 1500 modes is useful for low-timing-jitter line-by-line waveform generation and astronomical referencing, where the large mode spacing and absolute frequency stability are critical [3,5,6]. Furthermore, the same techniques demonstrated here should be generally applicable with any mode-locked laser in the visible and near-IR spectral regions.

The experiment employs an octave-spanning (550 nm to 1100 nm) Ti:sapphire frequency comb with a repetition rate of 1 GHz (Fig. 1) [11]. A standard f–$2f$ interferometer is used to detect the offset frequency for locking. The wavelength region near 657 nm is used to lock the comb to a stable cw optical reference or to detect the repetition rate for locking to a microwave frequency standard. In the case of the optical reference, this approach yields comb linewidths at the ~1 Hz level and subfemtosecond timing jitter [11]. Chen *et al.* have shown that cavity filtering causes a minimal increase in timing jitter [9].

The remainder of the spectrum (800 nm to 1050 nm) is reflected six times off planar mirrors with the same coating as the mirrors of the filter cavity to reduce the out-of-band light incident on the cavity. The beam is then sent through a polarizer and into the cavity, which has a mirror separation of ~7.5 mm. A standard dither lock is employed that overlaps the cavity resonances with every twentieth 1 GHz comb mode, yielding a filtered mode spacing of 20 GHz. We implement the double-pass cavity by retroreflecting the single-pass cavity light back into the cavity with a curved mirror (see Fig. 1). A broadband Faraday isolator without an input polarizer rotates the light to the orthogonal polarization for the second pass through the cavity. The use of an isolator instead of a quarter-wave plate was found to be critical to mitigate coupled cavity effects.

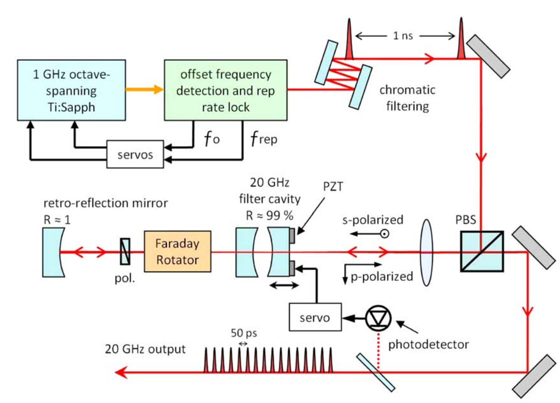

Fig. 1. (Color online) Stabilized 1 GHz input frequency comb is filtered by double passing through a 20 GHz FP cavity. The 20 GHz cavity is locked to the comb using a piezoelectric tranducer behind one of the mirrors.

Careful consideration is given to the choice of cavity mirrors to yield broad bandwidth and high suppression of unwanted modes. Although suppression (defined as the ratio between the intensity transmission of an on-resonant mode and its nearest off-resonant neighbor) improves with finesse, the accompanying dispersion and narrower cavity linewidth decrease the usable bandwidth. The narrower the cavity linewidth is, the more sensitive the coupling is to cumulative phase walk-off (dispersion), so the optimal cavity mirrors require a compromise between high reflectivity and coupling bandwidth [4,6].

To illustrate this trade-off, we model a FP cavity consisting of two quarter-wave stack mirrors spaced by $L=7.5$ mm. Quarter-wave stack dielectrics provide the simplest route to low-loss low-dispersion mirrors of high reflectivity and can be easily analyzed. We evauluate standard equations for the characteristic matrix of a quarter-wave stack composed of a fused-silica substrate and N pairs of high- and low-index quarter-wave layers ($n_H=2.2$, $n_L=1.46$, $\lambda/4$ centered at 900 nm) [12]. The reflectivity and phase shifts are calculated for $N=7$ through $N=13$ layer pairs. Using these calculations, the coupling bandwidth and nearest-neighbor suppression are calculated for a 1 GHz frequency comb filtered by a 20 GHz cavity. The $\lambda_0=900$ nm mode is aligned with the center of the cavity mode; however, the unequally spaced cavity modes will walk off of the comb modes after a certain bandwidth because of dispersion in the mirrors.

Figure 2 shows that suppression is increased at the cost of decreased coupling bandwidth; however, the suppression can be doubled (on a log scale) by double passing the FP cavity with only a 5% to 15% decrease in coupling bandwidth. Therefore, a much higher bandwidth can be achieved with a double-pass cavity for the same suppression of off-resonant modes. For example, to obtain 60 dB of off-resonant mode suppression, a single-pass cavity will require a finesse of around 10^4 and have a bandwidth of ~80 nm (Fig. 2 right dotted ellipse), while a double-pass cavity will require a finess of around 400 and have a bandwidth of ~160 nm (Fig. 2 left dotted ellipse). For this reason, we have chosen to employ a moderate finesse cavity (~300) in a double-pass configuration to achive high suppression and a large coupling bandwidth. For our desired applications the optimum value is $R=99\%$ centered at 900 nm [4].

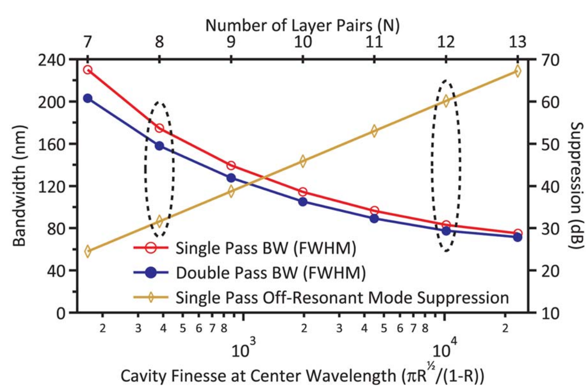

Fig. 2. (Color online) Simulation of quarter-wave stack mirrors and associated FP cavities. The coupling bandwidth (BW) decreases with increasing cavity finesse owing to the increased sensitivity to dispersion. Double-pass suppression is not shown, as it is exactly double the single-pass suppression, e.g., 60 dB versus 30 dB.

We examine the spectral and temporal properties of the output from the filtering cavity in both single- and double-pass configurations.

The bandwidth of efficient coupling for the single-pass and double-pass cavities are 124 nm and 104 nm, respectively [Fig. 3(a)]. This is less than the bandwidth predicted by our simulation, because the input spectrum is centered around 960 nm. Since the cavity locks to the highest power throughput, the lock centers around this peak. The FP simulation showed a similar decrease in bandwidth for locking the cavity 60 nm away from the center of the mirror reflection bandwidth. The input power at 1 GHz is 250 mW, and the output power at 20 GHz for the single-pass cavity is 6.5 mW, while the ouput for the double-pass cavity is 4.5 mW. This compares with the 12.5 mW that would be expected if the cavity selected one of every 20 optical modes without additional loss. Much of the loss for the single-pass case is due to the nonideal spatial mode of the input light from the octave spanning laser, while most of the additional loss for the second pass results from the isolator.

A significant advantage of the double-pass geometry is the doubling in suppression of unwanted (off-resonant) modes. While microwave measurements with a fast photodiode yield information about this suppression, the most accurate measurement is via heterodyne detection. The heterodyne beat of the 20 GHz comb with a cw laser at 960 nm directly yields the powers in individual comb modes. Examples are shown in Fig. 4.

The single-pass cavity shows 27 dB of off-resonant mode suppression, while the double-pass cavity provides 50 dB of off-resonant mode suppression. The impact of this off-resonant mode suppression is

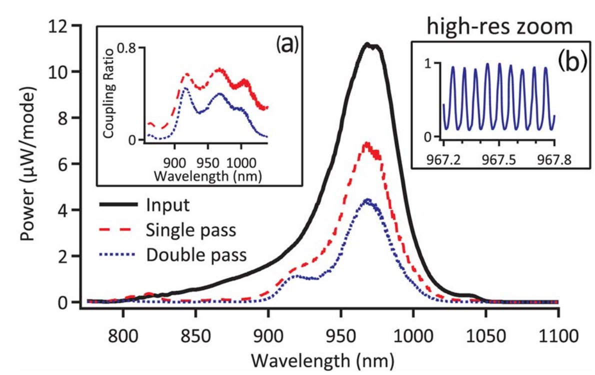

Fig. 3. (Color online) Input and output spectra for single- and double-pass cavities (power per mode). Most of the input bandwidth (50 nm FWHM) is coupled for both cases, giving output bandwidths of ~40 nm (FWHM). (a) Coupling ratio of output over input power per mode. Single pass shows 124 nm (FWHM) coupling bandwidth. Double pass shows 104 nm (FWHM) coupling bandwidth. (b) Zoomed view of high resolution (0.02 nm) optical spectrum analyzer trace showing individually resolved modes at 20 GHz.

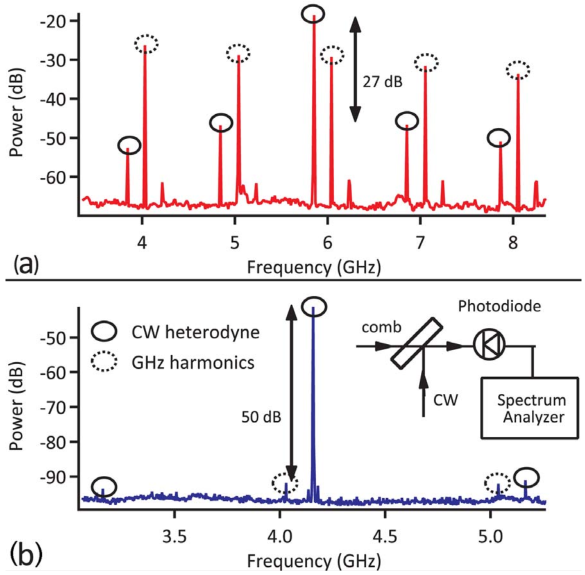

Fig. 4. (Color online) (a) Heterodyne beat with the single-pass cavity output. In addition to the beat notes indicated by solid circles, harmonics of the 1 GHz repetition rate are evident, as indicated by the dotted circles. The largest peak in the figure is the beat of the cw laser against a comb tooth aligned to the cavity resonance. The off-resonant comb teeth are suppressed by 27 dB. (b) cw heterodyne beat with the double-pass cavity output. The off-resonant mode suppression is 50 dB.

clearly seen in the time-domain waveforms of Fig. 5. Here the output of the 20 GHz cavity filter was detected with a 45 GHz photodiode and displayed on a 50 GHz oscilloscope.

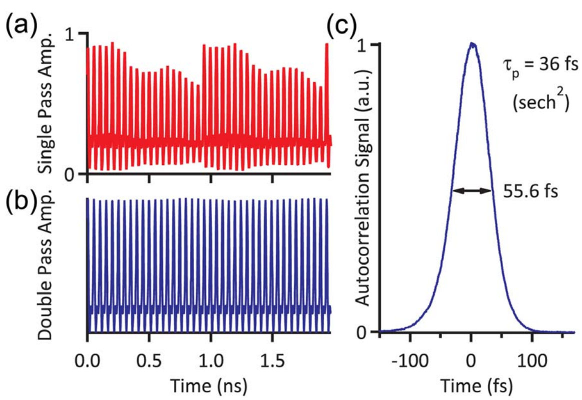

Fig. 5. (Color online) (a) Single-pass cavity time-domain signal with 30% amplitude modulation caused by the transmission of off-resonant comb modes. (b) Double-pass cavity time-domain signal showing less than 2% modulation. (c) Intensity autocorrelation trace showing a pulse width of 36 fs after compression by SF10 prisms. The transform limit is 30 fs.

The single-pass cavity shows more than 30% amplitude modulation at the original 1 GHz repetition rate, while the double-pass cavity shows less than 2% amplitude modulation. Figure 5(c) shows the autocorrelation of the 20 GHz pulses, which have been compressed to a duration of less than 40 fs. Applications such as pulse shaping will introduce inevitable losses, so we have additionally employed a broadband semiconductor optical amplifier at 980 nm that provides up to 20 dB of gain. With this we have amplified the 20 GHz comb after a shaper from ~100 μW up to 5 mW while still maintaining pulses as short as 60 fs with a bandwidth of 30 nm.

This high-fidelity 20 GHz frequency comb produced with the double-pass cavity is appropriate for the applications mentioned above. In particular, the precise frequency control and broad bandwidths should enable line-by-line femtosecond optical waveform generation with controlled carrier-envelope phase.

Since submission of this work, we have become aware of a related paper describing approaches to cavity-filled optical frequency combs [13].

References

1. A. M. Weiner, Rev. Sci. Instrum. **71**, 1929 (2000).
2. A. M. Weiner, D. E. Leaird, G. P. Wiederrecht, and K. A. Nelson, Science **247**, 1317 (1990).
3. Z. Jiang, C. Huang, D. E. Leaird, and A. M. Weiner, Nat. Photonics **1**, 463 (2007).
4. S. A. Diddams, M. S. Kirchner, T. Fortier, D. Braje, A. M. Weiner, and L. Hollberg, Opt. Express **17**, 3331 (2009).
5. M. T. Murphy, Th. Udem, R. Holzwarth, A. Sizmann, L. Pasquini, C. Araujo-Hauck, H. Dekker, S. D'Odorico, M. Fischer, T. W Hänsch, and A. Manescau, Mon. Not. R. Astron. Soc. **380**, 839 (2007).
6. D. A. Braje, M. S. Kirchner, S. Osterman, T. Fortier, and S. A. Diddams, Eur. Phys. J. D **48**, 57 (2008).
7. D. J. Jones, S. A. Diddams, J. K. Ranka, A. Stentz, R. S. Windeler, J. L. Hall, and S. T. Cundiff, Science **288**, 635 (2000).
8. T. Sizer, IEEE J. Quantum Electron. **25**, 97 (1989).
9. J. Chen, J. W. Sickler, P. Fendel, E. P. Ippen, F. X Kärtner, T. Wilken, R. Holzwarth, and T. W Hänsch, Opt. Lett. **33**, 959 (2008).
10. K. Yiannopoulos, K. Vyrsokinos, E. Kehayas, N. Pleros, K. Vlachos, H. Avramopoulos, and G. Guekos, IEEE Photon. Technol. Lett. **15**, 1294 (2003).
11. T. M. Fortier, A. Bartels, and S. A. Diddams, Opt. Lett. **31**, 1011 (2006).
12. M. Born and E. Wolf, *Principles of Optics* (Cambridge U. Press, 1980).
13. T. Steinmetz, T. Wilken, C. Araujo-Hauck, R. Holzwarth, T. W. Hänsch, and T. Udem, Appl. Phys. B (to be published).